Oxo Complexes

DOI: 10.1002/ange.201002733

A Low-Spin Ruthenium(IV)–Oxo Complex: Does the Spin State Have an Impact on the Reactivity?**

Takahiko Kojima, Yuichirou Hirai, Tomoya Ishizuka, Yoshihito Shiota, Kazunari Yoshizawa, Kenichiro Ikemura, Takashi Ogura, and Shunichi Fukuzumi**

High-valent metal–oxo complexes are key reactive species for oxidation and oxygenation of organic compounds in nature as well as in the laboratory.[1,2] Although iron is the most common metal species among high-valent metal–oxo complexes,[3] there are also manganese–oxo,[4] ruthenium–oxo,[5] and other metal–oxo complexes.[6] High-valent metal–oxo species are produced by reductive activation of molecular oxygen coupled with proton transfer.[7–9] Peroxides such as hydrogen peroxide can provide a so-called "peroxide shunt" to produce high-valent metal–oxo species.[1–3] High-valent metal–oxo species can also be produced by proton-coupled electron transfer (PCET), in which deprotonation of a coordinated water molecule and oxidation of the metal center occur concertedly.[10–14] The reactivity of high-valent metal–oxo species varies depending on the type of metal, the oxidation state of the metal center, ligands, and the spin state. Theoretical studies proposed that the reactivity of high-valent metal–oxo species may be determined by two closely lying spin states, which have different activation barriers for the reactions with substrates.[15–17] The most straightforward way to clarify the effects of spin states on the reactivity of high-valent metal–oxo species is to examine the reactivity of an analogous series of metal–oxo complexes that have different spin states. There have been extensive studies on Ru^{IV}–oxo complexes that exhibit the triplet spin state ($S=1$).[18–20] However, there has been no example of Ru^{IV}–oxo complexes exhibiting the singlet spin state ($S=0$) at the ground state.[21] Thus, comparison of the reactivity of analogous high-valent metal–oxo species with different spin states has never been made.

We report herein for the first time the spin state alteration of Ru^{IV}–oxo complexes with tris(2-pyridylmethyl)amine (tpa) derivatives depending on the type of tpa derivatives. Two Ru^{II}–aqua complexes having tpa derivatives, tetradentate tpa and a pentadentate *N*,*N*-bis(2-pyridylmethyl)-*N*-(6-carboxylato-2-pyridyl-methyl)amine (6-COO^--tpa) monoanion, $[Ru(tpa)(H_2O)_2]^{2+}$ (**1**)[13] and $[Ru(6\text{-}COO^-\text{-}tpa)(H_2O)]^+$ (**2**), were converted into the corresponding Ru^{IV}–oxo complexes by the PCET reactions with use of $(NH_4)_2[Ce^{IV}(NO_3)_6]$ (CAN) as an oxidant. Now we have two kinds of Ru^{IV}–oxo complexes, $[Ru(O)(tpa)(H_2O)]^{2+}$ (**3**) in the $S=1$ spin state and $[Ru(O)(6\text{-}COO^-\text{-}tpa)]^+$ (**4**) in the $S=0$ spin state. Thus, analogous Ru^{IV}–oxo complexes with different spin states in hand provide an excellent opportunity to compare the reactivity toward substrates in light of their spin states.

The Ru^{II}–aqua complex **2** was prepared by the reaction of a precursor complex $[Ru(6\text{-}COO^-\text{-}tpa)Cl]PF_6$ (see Figure 1)[22] with $AgPF_6$ in water by dechlorination and spontaneous reduction. UV/Vis spectroscopic titration on **2** revealed two-step deprotonation in 0.1 M Britton–Robinson buffer with 10 M NaOH solution. The first deprotonation process was reversible, and the pK_a value was determined to be 3.5 (Figure S1 in Supporting Information).[23]

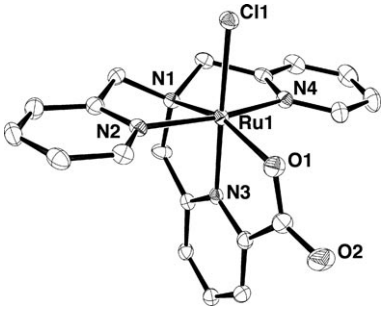

Figure 1. Crystal structure of the cationic moiety of $[Ru(6\text{-}COO^-\text{-}tpa)Cl]ClO_4$ with selected atom labeling. Each atom is described with thermal ellipsoids at the 50% probability level. Hydrogen atoms are omitted for clarity.

[*] Prof. Dr. T. Kojima, Dr. T. Ishizuka
Department of Chemistry, Graduate School of Pure and Applied Sciences, University of Tsukuba
1-1-1 Tennoudai, Tsukuba, Ibaraki 305-8571 (Japan)
Fax: (+81) 29-853-4323
E-mail: kojima@chem.tsukuba.ac.jp
Y. Hirai, Prof. Dr. S. Fukuzumi
Department of Material and Life Science, Osaka University
2-1 Yamada-oka, Suita, Osaka 565-0871 (Japan)
and
Department of Bioinspired Science, Ewha Womans University
Seoul, 120-750 (Korea)
Fax: (+81) 6-6879-7370
E-mail: fukuzumi@chem.eng.osaka-u.ac.jp
Dr. Y. Shiota, Prof. Dr. K. Yoshizawa
Institute for Materials Chemistry and Engineering
Kyushu University, Moto-oka, Nishi-Ku, Fukuoka 819-0395 (Japan)
Dr. K. Ikemura, Prof. Dr. T. Ogura
Graduate School of Life Science, University of Hyogo
Kouto, Hyogo 678-1297 (Japan)

[**] This work was supported by Grants-in-Aids (Nos. 20108010 (S.F.) and 21350035 (T.K.)) from the Japan Society of Promotion of Science (JSPS), MEXT, Japan (No. 20050029 to T.O. on Priority Area 477), and KOSEF/MEST through WCU project (R31-2008-000-10010-0).

Supporting information for this article is available on the WWW under http://dx.doi.org/10.1002/anie.201002733.

Complex **2** showed a reversible redox couple assigned to the Ru^{III}/Ru^{IV} couple at +0.68 V (vs. SCE), which was intact in the pH range 2–4 in Britton–Robinson buffer at room temperature (Figure S2 in the Supporting Information). In light of the redox potential (1.0 V vs. SCE at pH 0)[13] of CAN in H_2O, **2** should be converted into a Ru^{IV}–oxo complex by the oxidation with CAN.

Oxidation of **2** by CAN in water gave rise to the formation of a Ru^{IV}–oxo complex (**4**). In the course of the oxidation, we observed the absorption spectral change as shown in Figure S3 (see the Supporting Information). Resonance Raman spectroscopy allowed us to observe a Raman scattering due to the ν(Ru=O) vibration at 833 cm^{-1}, and this signal shifted to 788 cm^{-1} in the preparation in $H_2{}^{18}O$ (see Figure S4 in the Supporting Information). The isotopic shift is consistent with the calculated value for the Ru=O harmonic oscillator ($\Delta\nu$ = 40 cm^{-1}), supporting the formation of the Ru^{IV}=O species. ESIMS analysis allowed us to observe a peak cluster at *m*/*z* 451.11 (calcd 451.03) assigned to **4** in $H_2{}^{16}O$. The reaction of **2** with CAN in $H_2{}^{18}O$ gave a mixture of **4** and ^{18}O-labeled **4** (1.0:0.9) owing to slow exchange of the aqua ligand (see Figure S5 in the Supporting Information).

Ru^{IV}–oxo complex **4** was also characterized by ^1H NMR spectroscopy (Figure S6 in the Supporting Information). We observed an AB quartet at δ = 5.52 and 5.93 ppm (J_{AB} = 16 Hz), assigned to the equatorial CH_2 moieties, and a singlet at δ = 5.81 ppm due to the axial CH_2 moiety. Complex **4** showed a diamagnetic spectrum, indicating the retention of the σ_h symmetry in the precursor chlorido complex, which is in sharp contrast to the paramagnetically shifted signals of **2** (S = 1).[13] Thus, the spin state of **4** was determined to be S = 0, and, to the best of our knowledge, this is the first example of a low-spin Ru^{IV}–oxo complex.

DFT calculations at the B3LYP/LANL2DZ level of theory suggested that the structure of **4** should be pentagonal bipyramidal with a plane of symmetry (*Cs* symmetry). An optimized structure is depicted in Figure 2. It was also revealed that hydrogen bonding with water molecules should be indispensable to stabilize the singlet state over the triplet state: Without hydrogen-bonded water molecule(s), the triplet state should be dominant (Table S1 in the Supporting Information). Thus, water molecules play an important role to stabilize the singlet state of the Ru^{IV}=O species in water. In the optimized structure of **4**, the length of Ru^{IV}=O bond is 1.813 Å and that for the aqua ligand, Ru^{IV}–OH_2, is 2.265 Å. Thus, the formulation of low-spin **4** should be $[Ru(O)(6\text{-}COO^{-}\text{-}tpa)(H_2O)]^{2+}$ in water.

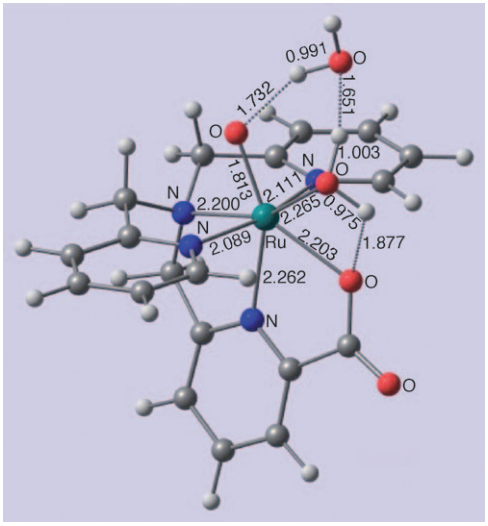

Figure 2. An optimized structure of **4** with hydrogen-bonded water molecules obtained by DFT calculations at the B3LYP/LANL2DZ level of theory.

Ru^{II}–aqua complexes **1** and **2** were applied to catalytic oxygenation of organic substrates under conditions in which substrates (0.1 M), CAN (0.2 M), and a catalyst (1 mM) (molar ratio 100:200:1) were mixed in D_2O (1 mL). The reaction mixture was stirred at room temperature for 1 h, and the product was quantified by ^1H NMR spectroscopy on the basis of peak integration. To demonstrate the reactivity of catalytic systems using those complexes toward various substrates, three types of substrates, namely, cyclohexene (olefin), 1-propanol (alcohol), and 4-sulfonate-1-ethylbenzene (saturated C-H), were examined. Regardless of the spin states of the Ru^{IV}=O species, the product distribution in the two systems was identical for each substrate as summarized in Table 1. Catalytic oxygenation of cyclohexene resulted in the formation of adipic acid as an eight-electron oxidation product. The selectivity of the catalytic cyclohexene oxygenation with the use of **2** as a catalyst was slightly lower in the presence of a twofold molar amount of the oxidant relative to the substrate than that found in the reaction with **1**; however, the selectivity was much improved with the use of an eightfold molar amount of CAN relative to cyclohexene to give adipic acid as the sole product. Oxygenation of 1-propanol led to the selective formation of propionic acid.[24] Oxygenation of saturated C–H bonds was also observed for both catalysts. All reactions should proceed via formation of Ru^{IV}–oxo species as reactive species as described above. As no significant difference in selectivity and efficiency was observed for the two complexes, the differences in ligands and spin states of catalysts have no significant influence on their catalytic activities.

Table 1: Catalytic oxidation reactions of organic substrates with **1** and **2** as catalysts.[a]

Entry	Substrate	Cat.	Product	Sel. [%]	Ox. eff. [%]	TON
1		**1**	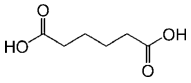	100	100	25
2		**2**		88	88	22
3	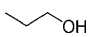	**1**		100	100	50
4		**2**		92	92	46
5	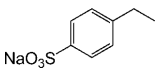	**1**	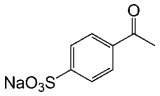	100	89	45
6		**2**		89	94	47

[a] [Substrate] = 0.1 M, [CAN] = 0.2 M, and [catalyst] = 1 mM.

To shed light on the detailed oxidation mechanism, we conducted kinetic analysis on the oxidation of 1-propanol with Ru^{IV}–oxo complexes **3** and **4** by a spectroscopic method. Addition of excess 1-propanol (150 mM) into aqueous solutions of the oxo complexes **3** and **4** (0.1 mM) gave continuous spectral change with isosbestic points (Figure 3a,b). In Figure 3a, as the reaction proceeds, the absorption band due to **3** ($\lambda_{max} \approx 450$ nm) decreases and the absorption band due to Ru^{II} ($\lambda_{max} = 624$ nm) increases. The time course of the absorbance at $\lambda = 624$ and 450 nm obeyed first-order kinetics and the pseudo-first-order rate constants obtained by the rise at $\lambda = 624$ nm and the decay at $\lambda = 450$ nm were the same. Similar behavior was observed for the spectra of **4** (Figure 3b). As the reaction proceeds, the absorption band due to Ru^{IV} ($\lambda_{max} = 542$ nm) decreases and the absorption band due to Ru^{II} ($\lambda_{max} = 628$ nm) increases.

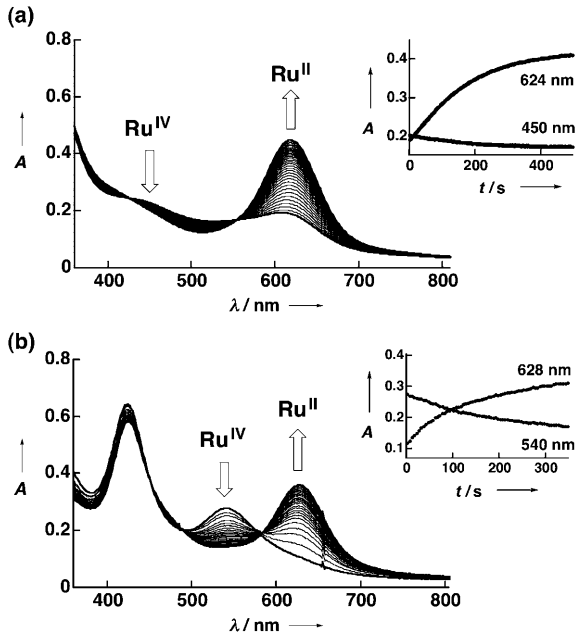

Figure 3. Spectral changes in the oxidation of 2-propanol with a) **3** and b) **4** in water.

Pseudo-first-order rate constants (k_{obs}) were determined with various concentrations of 1-propanol. The results for **3** and **4** are summarized in Figures S7 and S8 (see the Supporting Information), respectively. In the oxidation of 1-propanol, saturation behavior of rate constants with respect to concentration of 1-propanol was observed for both **3** and **4**. This behavior indicates the existence of pre-equilibrium prior to the oxidation reaction. Thus, it is suggested that there is interaction between the substrate and the oxo complexes prior to the oxidation reaction. Plots of k_{obs} versus the concentration of 1-propanol ([Sub]) were fitted by Equation (1).[25]

$$k_{obs} = kK[\mathrm{Sub}]/(1 + K[\mathrm{Sub}]) \quad (1)$$

The curve fitting affords equilibrium constants (K) of the pre-equilibrium and the rate constants (k) of the oxidation reaction in the precursor complexes. In the oxidation of 1-propanol with **3** at 301 K, those values were determined to be $K = 28\,\mathrm{M}^{-1}$ and $k = 5.7 \times 10^{-3}\,\mathrm{s}^{-1}$. Similarly, in the case of **4**, they were determined to be $K = 58\,\mathrm{M}^{-1}$ and $k = 5.6 \times 10^{-3}\,\mathrm{s}^{-1}$. Saturation behavior was also observed in all temperatures regardless of difference in Ru complexes. The kinetic data are summarized in Table 2.

Table 2: Equilibrium constants and rate constants for oxidation of 1-propanol with **2** and **4** at various temperatures.

	3		**4**	
T [K]	K [M^{-1}]	$10^3 k$ [s^{-1}]	K [M^{-1}]	$10^3 k$ [s^{-1}]
308	25 ± 2	10.3 ± 0.3	45 ± 3	8.1 ± 0.2
301	28 ± 3	5.7 ± 0.2	58 ± 5	5.6 ± 0.1
288	33 ± 3	3.8 ± 0.05	97 ± 6	2.9 ± 0.02
280	37 ± 2	2.5 ± 0.02	188 ± 6	1.9 ± 0.01

Temperature dependence of the formation constants and the rate constants was also investigated to obtain van't Hoff plots and Eyring plots, respectively. These plots allowed us to determine thermodynamic parameters to discuss on the oxidation reaction mechanism. On the basis of the van't Hoff plots (Figure S9 in the Supporting Information), the thermodynamic parameters were determined to be $\Delta H = -9.9 \pm 0.4\,\mathrm{kJ\,mol^{-1}}$ and $\Delta S = -5.0 \pm 1.3\,\mathrm{J\,K^{-1}\,mol^{-1}}$ (301 K) for **3** and $\Delta H = -36 \pm 4\,\mathrm{kJ\,mol^{-1}}$ and $\Delta S = -84 \pm 14\,\mathrm{J\,K^{-1}\,mol^{-1}}$ (301 K) for **4**. Thus, the formation of the precursor complexes is always exothermic and stabilization of the complex may result from the formation of hydrogen bonding between 1-propanol and the Ru^{IV}–oxo complexes.

We made efforts to obtain a direct evidence to support the two-step reaction including the pre-equilibrium in the oxidation of 1-propanol by **4**. To observe the fast first-step reaction, stopped-flow techniques were applied to separate the two-step reaction. As the result of measurements, we obtained two-step spectral changes with different isosbestic points as shown in Figure 4. The first reaction completed within 5 s, exhibiting an isosbestic point at $\lambda = 593$ nm (Figure 4, left). In addition, initial absorption maximum at $\lambda = 542$ nm shifted to $\lambda = 539$ nm in the course of the reaction (Figure 4, left; inset). In the second step, the reaction proceeded with an isosbestic point at $\lambda = 580$ nm (Figure 4, right). Thus, we concluded that the oxidation of 1-propanol with **4** consists of two steps, that is, formation of the putative hydrogen-bonding complex and the subsequent oxidation reaction in the complex.

The temperature dependence of the rate constants for the oxidation of 1-propanol with **3** and **4** (Table 3) allowed us to determine the activation parameters to shed some lights on the transition state of the oxidation reaction from Eyring plots as shown in Figure S10 (see the Supporting Information). For both Ru^{IV}–oxo complexes, similar activation parameters were obtained: $\Delta H^{\neq} = 31 \pm 4.7\,\mathrm{kJ\,mol^{-1}}$ and $\Delta S^{\neq} = -184 \pm 16\,\mathrm{J\,K^{-1}\,mol^{-1}}$ for **3**, $\Delta H^{\neq} = 34 \pm 0.8\,\mathrm{kJ\,mol^{-1}}$ and $\Delta S^{\neq} = -174 \pm 2.5\,\mathrm{J\,K^{-1}\,mol^{-1}}$ for **4**. These similar activation parameters lend credence to a similar transition state for both Ru^{IV}–oxo complexes. Since the activation entropies are remarkably negative, the Ru^{IV}–oxo complexes are assumed to interact

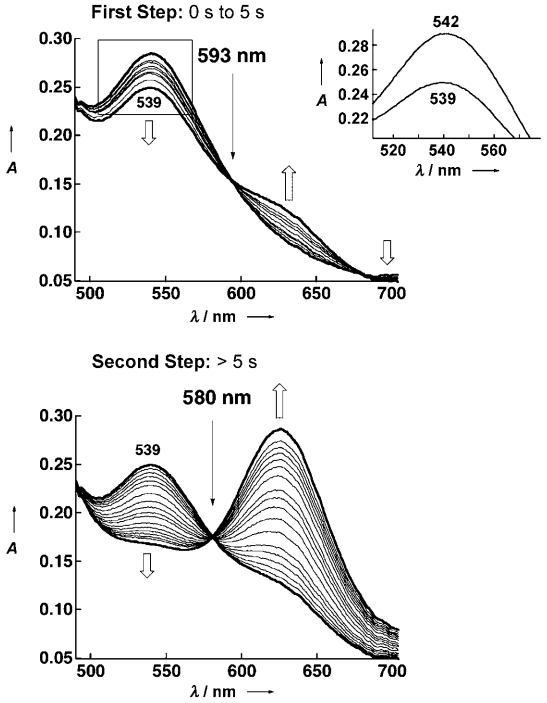

Figure 4. Two-step spectral changes in the reaction of 1-propanol (1.5×10^{-1} M) with **4** (1.0×10^{-4} M) at 288 K obtained by stopped-flow measurements. The bottom trace at 539 nm in the left is identical to the top trace in the right.

Table 3: Kinetics data for reactions of 1-propanol with Ru^{IV}–oxo complexes **3** and **4**.

Complex	ΔH [kJ mol^{-1}]	ΔS [J K^{-1} mol^{-1}]	$\Delta H^{\neq}$ [kJ mol^{-1}]	$\Delta S^{\neq}$ [J K^{-1} mol^{-1}]	k_H/k_D
3	-9.9 ± 0.4	-5.0 ± 1.3	31 ± 4.7	-184 ± 16	2.9
4	-36 ± 4	-84 ± 14	34 ± 0.8	-174 ± 2.5	2.1

strongly with the substrate to form tight transition states in the course of the dehydrogenation reaction.

To gain information on the hydrogen-abstraction process, we conducted kinetic experiments using $CH_3CH_2CD_2OH$ to evaluate kinetic isotope effects (KIEs). A significant difference in the rate constants was observed at 301 K (Figure S11 in the Supporting Information). KIE values for the observed maximum rate constants of **3** and **4** were determined to be 2.9 and 2.1, respectively.[26] This result indicates that the removal of the α-hydrogen atom is involved in the rate-determining step. In contrast, no kinetic isotope effect was observed for the hydrogen atom of the OH group, as indicated by comparison of the rate constant for the oxidation of $CH_3CH_2CH_2OD$ in D_2O. Thus, the rate-determining step lies in the hydrogen-abstraction process at the α-position of 1-propanol.

There are two possible mechanisms: one-step hydride transfer or proton-coupled electron transfer (PCET). Because there was no difference in reactivity between **3** with $S=1$ and **4** with $S=0$, the one-step hydride transfer, which is spin-forbidden for **3** to give the singlet product, is unlikely to occur. Thus, a PCET mechanism, which is spin-allowed irrespective of the spin state of **3** and **4**, may be operative in the oxidation of substrates with **3** and **4**.

All the kinetics data including heats and entropies of formation of the hydrogen-bonding complex, activation parameters, and kinetic isotope effects are summarized in Table 3. In comparative experiments between **3** and **4**, no meaningful difference was recognized, which clearly indicates that difference in the ligand or the spin state of the metal center of the oxo species does not affect their reactivity. This is the first example to clarify relationship between the spin state and the reactivity of high-valent metal–oxo species experimentally. The α-C–H bond in the hydrogen-bonded substrate is oriented to the oxo ligand to undergo PCET to give rise to a tightly condensed transition state as reflected on the negatively large activation entropy given in Table 3.

In summary, we have described detailed mechanistic insights into catalytic oxygenation and oxidation reactions by two Ru^{II}–aqua complexes with use of CAN as an oxidant in an acidic aqueous solution. The two aqua complexes afford Ru^{IV}–oxo complexes by the oxidation with CAN. Complex **2** with 6-COO^--tpa affords a low-spin Ru^{IV}–oxo complex ($S=0$), which is in sharp contrast to complex **1** with tpa, which gives an intermediate-spin Ru^{IV}–oxo complex ($S=1$). We have experimentally clarified for the first time that the spin state of the Ru^{IV}–oxo complexes does not affect their reactivity toward external substrates in oxygen atom transfer and hydrogen abstraction in water. In the detailed mechanistic investigation on 1-propanol oxidation, we have revealed that the formation of hydrogen-bonding adducts between the Ru=O complexes and the substrate occurs to gain high selectivity and efficiency in the oxidation reactions through a PCET mechanism. The results presented herein will provide new fundamentals of catalytic oxidation reactions by high-valent metal–oxo species in aqueous media.

Experimental Section

Synthesis of **2**: A solution containing [Ru^{III}(6-COO-tpa)Cl](PF_6) (50 mg, 0.081 mmol) and $AgPF_6$ (25 mg, 0.099 mmol) in H_2O (15 mL) was stirred until the color turned to green, and then heated to 60 °C for 2 h. The deep green solution was filtered through a membrane filter to remove insoluble solid. The filtrate was evaporated to remove solvent. 2-Propanol was then added to the flask to obtain a green precipitate. The precipitate was filtered and washed with diethyl ether and then dried in vacuo. The yield was 37 % (18 mg). ^{1}H NMR (D_2O): $\delta=5.62$ and 5.83 (ABq, $J_{AB}=16$ Hz, 4H, CH_2 (equatorial)), 5.70 (s, 2H, CH_2 (axial)), 7.71 (t, $J=6$ Hz, 2H, H5 of py(equatorial)), 7.77 (d, $J=8$ Hz, 1H, H3 of py(axial)), 7.95 (d, $J=8$ Hz, 2H, H3 of py(equatorial)), 8.2–8.3 (m, 4H, H4 of py(equatorial), H4 and H5 of py(axial)), 8.43 ppm (d, $J=6$ Hz, 2H, H6 of py(equatorial)). Absorption maxima in H_2O (λ_{max}, nm): 628, 410.

Received: May 6, 2010
Revised: July 27, 2010
Published online: September 23, 2010

Keywords: electronic structure · oxidation · oxo ligands · reaction mechanisms · ruthenium

[1] a) M. Sono, M. P. Roach, E. D. Coulter, J. H. Dawson, *Chem. Rev.* **1996**, *96*, 2841 – 2888; b) J. T. Groves, *Proc. Natl. Acad. Sci. USA* **2003**, *100*, 3569 – 3574; c) *Cytochrome P450: Structure, Mechanism and Biochemistry*, 3rd ed. (Ed.: P. R. Ortiz de Montellano), Kluwer Academic/Plenum, New York, **2004**.

[2] a) L. Que, Jr., *Acc. Chem. Res.* **2007**, *40*, 493 – 500; b) W. Nam, *Acc. Chem. Res.* **2007**, *40*, 522 – 531.

[3] J. T. Groves, Y. Watanabe, *J. Am. Chem. Soc.* **1988**, *110*, 8443 – 8452.

[4] a) V. K. Yachandra, K. Sauer, M. P. Klein, *Chem. Rev.* **1996**, *96*, 2927 – 2950; b) S. Fukuzumi, N. Fujioka, H. Kotani, K. Ohkubo, Y.-M. Lee, W. Nam, *J. Am. Chem. Soc.* **2009**, *131*, 17127 – 17134.

[5] a) T. Punniyamurthy, S. Velusamy, J. Iqbal, *Chem. Rev.* **2005**, *105*, 2329 – 2364; b) M. H. V. Huynh, T. J. Meyer, *Chem. Rev.* **2007**, *107*, 5004 – 5064; c) M. Sadakane, E. Stechhan, *Chem. Rev.* **1998**, *98*, 219 – 238.

[6] a) H. C. Kolb, M. S. VanNieuwenhze, K. B. Sharpless, *Chem. Rev.* **1994**, *94*, 2483 – 2547; b) A. Gunay, K. H. Theopold, *Chem. Rev.* **2010**, *110*, 1060 – 1081.

[7] S.-K. Lee, B. G. Fox, W. A. Froland, J. D. Lipscomb, E. Münck, *J. Am. Chem. Soc.* **1993**, *115*, 6450 – 6451.

[8] G. L. Berglund, G. H. Carlsson, A. T. Smith, H. Szöke, A. Henriksen, J. Hadju, *Nature* **2002**, *417*, 463.

[9] B. Meunier, S. P. de Visser, S. Shaik, *Chem. Rev.* **2004**, *104*, 3947 – 3980.

[10] a) C.-M. Che, V. W.-W. Yam, T. C. W. Mak, *J. Am. Chem. Soc.* **1990**, *112*, 2284 – 2291; b) J. A. Gilbert, D. S. Eggleston, W. R. Murphy, Jr., D. A. Geselowitz, S. W. Gersten, D. J. Hodgson, T. J. Meyer, *J. Am. Chem. Soc.* **1985**, *107*, 3855 – 3864; c) S. W. Gersten, G. J. Samuels, T. J. Meyer, *J. Am. Chem. Soc.* **1982**, *104*, 4029 – 4030.

[11] a) G. Süss-Fink, *Angew. Chem.* **2008**, *120*, 5972 – 5974; *Angew. Chem. Int. Ed.* **2008**, *47*, 5888 – 5890; b) T. J. Meyer, M. H. V. Huynh, *Inorg. Chem.* **2003**, *42*, 8140 – 8160.

[12] a) A. Sartorel, M. Carraro, G. Scorrano, R. de Zorzi, S. Geremia, N. D. McDaniel, S. Bernhard, M. Bonchio, *J. Am. Chem. Soc.* **2008**, *130*, 5006 – 5007; b) Y. V. Geletii, B. Botar, P. Kögerler, D. A. Hillesheim, D. G. Musaev, C. L. Hill, *Angew. Chem.* **2008**, *120*, 3960 – 3963; *Angew. Chem. Int. Ed.* **2008**, *47*, 3896 – 3899; c) W. W. Y. Lam, W.-L. Man, C.-F. Leung, C.-Y. Wong, T.-C. Lau, *J. Am. Chem. Soc.* **2007**, *129*, 13646 – 13652.

[13] Y. Hirai, T. Kojima, Y. Mizutani, Y. Shiota, K. Yoshizawa, S. Fukuzumi, *Angew. Chem.* **2008**, *120*, 5856 – 5860; *Angew. Chem. Int. Ed.* **2008**, *47*, 5772 – 5776.

[14] Y.-M. Lee, S. N. Dhuri, S. C. Sawant, J. Cho, M. Kubo, T. Ogura, S. Fukuzumi, W. Nam, *Angew. Chem.* **2009**, *121*, 1835 – 1838; *Angew. Chem. Int. Ed.* **2009**, *48*, 1803 – 1806.

[15] a) S. Shaik, H. Hirao, D. Kumar, *Acc. Chem. Res.* **2007**, *40*, 532 – 542; b) K. Yoshizawa, *Acc. Chem. Res.* **2006**, *39*, 375 – 382.

[16] a) S. N. Dhuri, M. S. Seo, Y.-M. Lee, H. Hirao, Y. Wang, W. Nam, W. S. Shaik, *Angew. Chem.* **2008**, *120*, 3404 – 3407; *Angew. Chem. Int. Ed.* **2008**, *47*, 3356 – 3359; b) H. Hirao, L. Que, Jr., W. Nam, S. Shaik, *Chem. Eur. J.* **2008**, *14*, 1740 – 1756.

[17] a) S. P. de Visser, *Angew. Chem.* **2006**, *118*, 1822 – 1825; *Angew. Chem. Int. Ed.* **2006**, *45*, 1790 – 1793; b) S. P. de Visser, *J. Am. Chem. Soc.* **2006**, *128*, 9813 – 9824; c) S. P. de Visser, *J. Am. Chem. Soc.* **2006**, *128*, 15809 – 15818; d) H. Hirao, D. Kumar, L. Que, Jr., S. Shaik, *J. Am. Chem. Soc.* **2006**, *128*, 8590 – 8606.

[18] a) B. A. Moyer, T. J. Meyer, *Inorg. Chem.* **1981**, *20*, 436 – 444; b) J. C. Dobson, W. K. Seok, T. J. Meyer, *Inorg. Chem.* **1986**, *25*, 1513 – 1514; c) L. Roecker, T. J. Meyer, *J. Am. Chem. Soc.* **1987**, *109*, 746 – 754.

[19] a) C.-M. Che, V. W. W. Yam, *J. Am. Chem. Soc.* **1987**, *109*, 1262 – 1263; b) C.-M. Che, W.-T. Tang, W.-T. Wong, T.-F. Lai, *J. Am. Chem. Soc.* **1989**, *111*, 9048 – 9056; c) C.-M. Che, C. Ho, T.-C. Lau, *J. Chem. Soc. Dalton Trans.* **1991**, 1901 – 1907.

[20] J. Benet-Buchholz, P. Comba, A. Llobet, S. Roeser, P. Vadivelu, H. Wadepohl, S. Wiesner, *Dalton Trans.* **2009**, 5910 – 5923.

[21] A low-spin and seven-coordinate Ru^{IV} complex: L. Duan, A. Fischer, Y. Xu, L. Sun, *J. Am. Chem. Soc.* **2009**, *131*, 10397 – 10399.

[22] See the Supporting Information for details. Crystallographic data for $[Ru(6\text{-}COO^{-}\text{-}tpa)Cl]ClO_4$: monoclinic, $P2_1/c$, $a = 10.750(2)$, $b = 14.734(2)$, $c = 14.526(2)$ Å, $\beta = 100.164(2)°$, $V = 2264.7(6)$ Å^3, $T = 123$ K, $Z = 4$, $R1(R_w) = 0.0449(0.1029)$ ($I > 2\sigma(I)$), GOF = 1.081. CCDC 772665 contains the supplementary crystallographic data for this paper. These data can be obtained free of charge from The Cambridge Crystallographic Data Centre via www.ccdc.cam.ac.uk/data_request/cif. *Caution:* Perchlorate salts of metal complexes with organic ligands are potentially explosive and should be handled with great care.

[23] The second deprotonation process was irreversible. We also observed formation of a red-colored μ-oxo Ru^{III} dimer under basic conditions. Details will be reported elsewhere.

[24] Complex **4**, formed by adding 2 equivalents of CAN to **2**, oxidized 1-propanol to afford the two-electron oxidized product, 1-propanal (propionaldehyde), as a main product and a small amount of propionic acid (ca. 12:1).

[25] a) E. A. Mader, E. R. Davidson, J. M. Mayer, *J. Am. Chem. Soc.* **2007**, *129*, 5153 – 5166; b) W. W. Y. Lam, M. F. W. Lee, T.-C. Lau, *Inorg. Chem.* **2006**, *45*, 315 – 321.

[26] Larger KIE values have been reported for benzyl alcohol oxidation by iron(IV)–oxo complexes: N. Y. Oh, Y. Suh, M. J. Park, M. S. Seo, J. Kim, W. Nam, *Angew. Chem.* **2005**, *117*, 4307 – 4311; *Angew. Chem. Int. Ed.* **2005**, *44*, 4235 – 4239.

